

Accelerated Publications

Structure of an Active Water Molecule in the Water-Oxidizing Complex of Photosystem II As Studied by FTIR Spectroscopy[†]

Takumi Noguchi^{*,‡} and Miwa Sugiura[§]

Biophysical Chemistry Laboratory, RIKEN (The Institute of Physical and Chemical Research), Wako, Saitama 351-0198, Japan, and Department of Applied Biological Chemistry, Faculty of Agriculture, Osaka Prefecture University, 1-1 Gakuen-cho, Sakai, Osaka 599-8531, Japan

Received May 8, 2000; Revised Manuscript Received July 5, 2000

ABSTRACT: The vibrations of a water molecule in the water-oxidizing complex (WOC) of photosystem II were detected for the first time using Fourier transform infrared (FTIR) spectroscopy. In a flash-induced FTIR difference spectrum upon the S₁-to-S₂ transition, a pair of positive and negative bands was observed at 3618 and 3585 cm⁻¹, respectively, and both bands exhibited downshifts by 12 cm⁻¹ upon replacement of H₂¹⁶O by H₂¹⁸O. Upon D₂O substitution, the bands largely shifted down to 2681 and 2652 cm⁻¹. These observations indicate that the bands at 3618 and 3585 cm⁻¹ arise from the O–H stretching vibrations of a water molecule, probably substrate water, coupled to the Mn cluster in the S₂ and S₁ states, respectively. The band frequencies indicate that the O–H group forms a weak H-bond and this H-bonding becomes weaker upon S₂ formation. Intramolecular coupling with the other O–H vibration of this water molecule was studied by a decoupling experiment using a H₂O/D₂O (1:1) mixture. The downshifts by decoupling were estimated to be 4 and 12 cm⁻¹ for the 3618 (S₂) and 3585 cm⁻¹ (S₁) bands, both of which were much smaller than 52 cm⁻¹ of water in vapor, indicating that the observed water has a considerably asymmetric structure; i.e., one of the O–H groups is weakly and the other is strongly H-bonded. The smaller coupling in the S₂ than the S₁ state means that this H-bonding asymmetry becomes more prominent upon S₂ formation. Such a structural change may facilitate the proton release reaction that takes place in the later step by lowering the potential barrier. The present study showed that FTIR detection of the O–H vibrations is a useful and promising method to directly monitor the chemical reactions of substrate water and clarify the molecular mechanism of photosynthetic water oxidation.

Photosynthesis is the process by which plants and certain types of bacteria convert the energy of light into the chemical energy of organic compounds such as sugars and starch. These energy-rich compounds are synthesized by reduction

of CO₂. As the source of electrons for this CO₂ reduction, plants and cyanobacteria use water, which is one of the most abundant resources on the earth. Hence, water works as a terminal electron donor in the electron-transfer chain of photosynthetic reactions. The oxidation of water is performed in the water-oxidizing complex (WOC),¹ which resides on the electron donor side of photosystem II (PSII) (1–6). The catalytic core of the WOC is a tetranuclear Mn cluster, whose structure has been proposed as a dimer of a di-μ-oxo dimer from EXAFS and EPR studies (3, 7). In the WOC, two water

[†] This research was supported by grants for the Photosynthetic Sciences and Biodesign Research Program at RIKEN given by the Science and Technology Agency (STA) of Japan.

^{*} To whom correspondence should be addressed.

[‡] RIKEN.

[§] Osaka Prefecture University.

molecules are oxidized to cleave into a O_2 molecule and four protons. This reaction proceeds through a light-driven cycle of five intermediates, S_0 – S_4 , in which the S_1 state is dark stable and O_2 is released in the S_4 -to- S_0 transition. As for the chemical mechanism of water oxidation, various models have been proposed so far (1–6). The general view is that (i) two substrate water molecules bind to Mn, (ii) protons are liberated in a stepwise or concerted way through the changes in the redox states of the Mn ions, and (iii) an O–O bond is created in the S_4 state and then O_2 is released. The current experimental knowledge, however, is so limited that the detailed chemical mechanism of water oxidation remains a mystery.

To clarify the mechanism of an enzymatic reaction, it is essential to probe a substrate molecule in the protein complex. In the case of the WOC, however, this is rather difficult because the substrate is water that is also the solvent of the system. The substrate water in the WOC must be distinguished from an enormous amount of bulk water. Up to now, several attempts have been made to detect water molecules bound to the Mn cluster. The NMR relaxation rate of solvent protons is enhanced by S-state changes, and this phenomenon was interpreted as due to rapid equilibrium between the protons of bulk water and those of Mn-coordinated water (8). Mass spectrometry studies indicated that the exchanging rate of water in the S_3 state is biphasic, and thus two substrate water molecules have strongly heterogeneous structures (9). Water binding to the Mn cluster has also been suggested by CW EPR studies, in which small changes were observed in the S_2 multiline signal in $H_2^{17}O$ (10) and D_2O (11). Britt (2) also showed the presence of water or hydroxo ligands to Mn in both the S_1 and S_2 states by ESEEM of D_2O -exchanged PSII particles. By contrast, in recent ESEEM investigations using $H_2^{17}O$ and D_2O -reconstituted PSII, Turconi et al. (12) could not obtain the evidence of H_2O binding to the Mn center giving rise to the multiline signal. In proton ENDOR studies, Kawamori et al. (13) and Fiege et al. (14) reported the protons from water ligands to the Mn cluster, whereas Tang et al. (15) did not observe signals from un-ionized water or hydroxo ligands directly bound to the Mn cluster.

We have been using FTIR difference spectroscopy to investigate the ligand and protein structures of the WOC (16–24). The FTIR spectra of the WOC have been obtained as light-induced difference spectra upon S_1 -to- S_2 transition. Analyses of the S_2/S_1 difference spectra have revealed the presence of carboxylate ligands (16–19, 23), the protonation and H-bonding structure of a histidine ligand (22), changes in conformations of the polypeptide chains (16, 18, 19), and the structural coupling of a tyrosine residue with the Mn cluster (21). Zhang et al. (25) and Chu et al. (26) recently reported S_2/S_1 or $S_2Q_A^-/S_1Q_A$ difference spectra in the 1800–1200 cm^{-1} region basically identical to ours. Chu et al. (26) further succeeded in measuring the lower frequency region

(1000–550 cm^{-1}) of those spectra, where the vibrations of di- μ -oxo-bridged Mn dimer are expected to be present.

Water has characteristic infrared absorption in the 3800–3000 cm^{-1} region that arises from its O–H stretching vibration. This vibration is the best monitor to study the structure and interactions of a water molecule, because it is highly sensitive to the H-bonding, metal binding, and molecular symmetry (27–33). It is also useful to directly detect the protonation and deprotonation reactions of water. As for water in proteins, Maeda, Kandori, and co-workers (34, 35) have extensively studied the structures of water molecules in the active sites of bacteriorhodopsin and rhodopsin by detecting the O–H stretching vibrations using a light-induced FTIR difference technique. These studies showed the interaction changes of water molecules that are located in the proton-transfer pathways. In the present study, we have applied the same technique to study the structure and reaction of substrate water in the WOC. We have succeeded, for the first time, in detecting O–H vibrations of an active water molecule in the WOC and obtained the structural information of this water including the H-bonding interaction and the structural symmetry.

MATERIALS AND METHODS

Oxygen-evolving PSII core complexes from the thermophilic cyanobacterium *Synechococcus elongatus*, in which the carboxyl terminus of the CP43 subunit was genetically histidine-tagged, were purified using Ni^{2+} -affinity column chromatography as described by Sugiura and Inoue (36). The typical value of oxygen-evolving activity of this PSII core was 2200 μmol (mg of Chl) $^{-1}$ h $^{-1}$ at 25 °C with ferricyanide as an exogenous electron acceptor (36). Depletion of the Mn cluster was performed by NH_2OH treatment according to Sugiura and Inoue (36). The PSII core complexes were suspended in 40 mM Mes–NaOH buffer (pH 6.5) containing 20 mM NaCl, 15 mM $CaCl_2$, 15 mM $MgCl_2$, 0.03% DM, and 25% glycerol and stored in liquid N_2 until use. Before FTIR measurements, the core complexes were resuspended in 10 mM Mes–NaOH (pH 6.0) buffer containing 50 mM sucrose, 5 mM NaCl, 5 mM $CaCl_2$, and 0.06% DM. For the replacement of $H_2^{16}O$ with $H_2^{18}O$, an aliquot of sample suspension was dried under N_2 gas flow followed by resuspension with the same volume of $H_2^{18}O$. This replacement procedure was repeated twice. The PSII core suspension in $H_2^{18}O$ buffer was then incubated at 10 °C overnight. It is noted that the present core sample prepared from a thermophilic cyanobacterium is highly stable and retains more than 90% of the original oxygen-evolving activity even after 8-day incubation at 20 °C (36). The PSII samples in D_2O and H_2O/D_2O (1:1) buffers were prepared by the replacement of the H_2O buffer with the D_2O and H_2O/D_2O (1:1) buffers by repetitive concentration and dilution procedures using Microcon-100 (Amicon). The sample was then incubated at 6 °C overnight. The above procedures of buffer replacement were performed in the dark, so that the WOC was poised basically in the S_1 state.

FTIR spectra were measured on a Bruker IFS-66/S spectrophotometer equipped with an MCT detector (EG&G JUDSON). S_2/S_1 FTIR difference spectra were measured as described previously (18, 19, 21, 22). An aliquot of the core suspension (6 mg of Chl/mL; 5 μL) was mixed with 4 μL

¹ Abbreviations: DM, *n*-dodecyl β -D-maltoside; ENDOR, electron nuclear double resonance; EPR, electron paramagnetic resonance; ESEEM, electron spin–echo envelope modulation; EXAFS, extended X-ray absorption fine structure; FTIR, Fourier transform infrared; H-bond, hydrogen bond; Mes, 2-(*N*-morpholino)ethanesulfonic acid; PSII, photosystem II; Q_A , primary quinone electron acceptor of PSII; Q_B , secondary quinone electron acceptor of PSII; WOC, water-oxidizing complex.

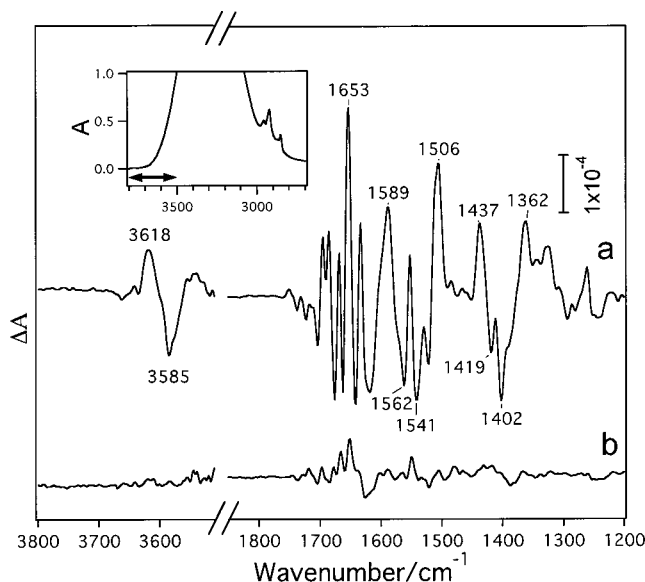


FIGURE 1: Flash-induced FTIR difference spectra upon S_1 -to- S_2 transition of the WOC in PSII core complexes from *S. elongatus* (a) and in Mn-depleted complexes (b). The samples included ferricyanide/ferrocyanide (1:9). Inset: FTIR absorption spectrum of the PSII core complexes in the O-H stretching region, in which the frequency region shown in difference spectra a and b is indicated by an arrow. The sample temperature was 250 K. Difference spectra were obtained as after-minus-before single-pulse illumination (532 nm; 7 ns). The spectral resolution was 4 cm^{-1} .

of ferricyanide/ferrocyanide (2 mM/18 mM) solution, lightly dried on a BaF_2 plate under N_2 gas flow, and covered with another BaF_2 plate. Absorbance of the amide I band around 1650 cm^{-1} was adjusted below 1.0. The sample temperature was kept at 250 K in a liquid N_2 cryostat (Oxford DN1704) equipped with a controller (Oxford ITC-5). Two single-beam spectra (200 s accumulation for each) were measured before and 10 s after single-pulse illumination from a frequency-doubled Nd:YAG laser (Quanta-Ray GCR-130) (532 nm; 7 ns pulse width; 20 mJ/pulse cm^2 at the sample point), and the difference spectrum was calculated by subtracting the spectrum obtained before illumination from that after illumination. The interval of 10 s after illumination was taken to complete the electron abstraction by ferricyanide on the electron acceptor side. The spectral resolution was 4 cm^{-1} . Six to eight spectra were averaged for final data.

RESULTS

Figure 1a shows a flash-induced S_2/S_1 FTIR spectrum of the WOC of the PSII core complexes from *S. elongatus*. The spectral features of the lower frequency region (1800–1200 cm^{-1}) follow those of the previously reported S_2/S_1 spectrum of PSII membranes of spinach (18, 19, 24) and PSII core complexes from *Synechocystis* PCC 6803 (21, 22). Several prominent bands are observed in the symmetric (1450–1350 cm^{-1}) and asymmetric (1600–1500 cm^{-1}) stretching regions of carboxylate groups, and complex structures appear in the amide I region (1700–1600 cm^{-1}). The sample included ferricyanide as an exogenous electron acceptor, and thus Q_A^-/Q_A or Q_B^-/Q_B signals, which are characterized by an intense CO stretching band of the semiquinone anion around 1480 cm^{-1} (25, 37, 38), were not observed. Instead, in the CN stretching region, positive and negative peaks at 2115 and

2038 cm^{-1} , respectively, appeared due to the reduction of ferricyanide to produce ferrocyanide (not shown). When the Mn cluster was depleted, most of the bands disappeared, leaving some weak signals (Figure 1b). These remaining signals are probably ascribed to the non-heme iron ($\text{Fe}^{2+}/\text{Fe}^{3+}$) (20, 39, 40), part of which is preoxidized even under the redox condition of ferrocyanide/ferricyanide (9:1) and hence becomes an endogenous electron acceptor. Bicarbonate seems to be released from this preoxidized non-heme iron, because the bands of bicarbonate at 1338 and 1228 cm^{-1} (39) are missing and the spectrum is more similar to that of the non-heme iron with glycolate (40). The disappearance of most bands by Mn depletion (Figure 1b) reinforced the idea that the spectrum of the Mn-intact PSII core complexes in Figure 1a arises from the WOC, although some contamination signals from the non-heme iron may be included. It is noted that, in Figure 1b, the Y_D/Y_D signals, which have been detected in the Mn-depleted PSII with ferricyanide (21, 38), were not observed. This is probably because ferrocyanide, which was included in the sample with high concentration (ferrocyanide:ferricyanide = 9:1), worked as an exogenous electron donor, and hence Y_D^* was not accumulated in this PSII.

The original FTIR spectrum of the PSII sample shows a strong absorption band around 3300 cm^{-1} , which is due to the strongly H-bonded O-H stretching vibrations of bulk water (ice in this case) (Figure 1, inset). Because a rather wet sample was used in this study to avoid inactivation of the WOC, infrared absorption in the 3500–3100 cm^{-1} region was saturated ($A > 1.0$) (Figure 1, inset), and hence the spectrum in this region was not available. On the other hand, the higher frequency region of 3800–3500 cm^{-1} , where free or weakly H-bonded O-H stretching bands of water occur, escaped from saturation (Figure 1 inset). Thus, a light-induced difference spectrum can be obtained in this frequency region. The S_2/S_1 spectrum in this high-frequency region is included in Figure 1a. There appeared prominent positive and negative bands at 3618 and 3585 cm^{-1} , respectively. The band intensities were comparable with those of the carboxylate bands in the 1600–1350 cm^{-1} region (Figure 1a). Both of the bands at 3618/3585 cm^{-1} disappeared upon Mn depletion (Figure 1b), confirming that these belong to the S_2/S_1 change of the WOC. A similar band pair was observed also in the S_2/S_1 difference spectrum of BBY-type PSII membranes from spinach (spectrum not shown), indicating that this signal is not specific to cyanobacteria or core preparations. It should be also noted that this observation, along with the spectral features in the 1800–1200 cm^{-1} region, similar to those of spinach membranes and *Synechocystis* core complexes, indicates that the His-tag of CP43 in this *S. elongatus* mutant does not affect the structure of the WOC detected by FTIR.

To examine whether the signal at 3618/3585 cm^{-1} arises from the O-H stretching vibrations of water, the spectrum was measured using the sample incubated in H_2^{18}O buffer. In the lower frequency region (1800–1200 cm^{-1}), the S_2/S_1 spectrum obtained (not shown) was virtually identical to that of the sample in H_2^{16}O (Figure 1a), indicating that the PSII sample was not damaged by the $\text{H}_2^{16}\text{O}/\text{H}_2^{18}\text{O}$ replacement procedure. The S_2/S_1 difference spectrum in the O-H region measured in the H_2^{18}O buffer is shown in Figure 2a (thick line) compared with that in the H_2^{16}O buffer (thin line). Both

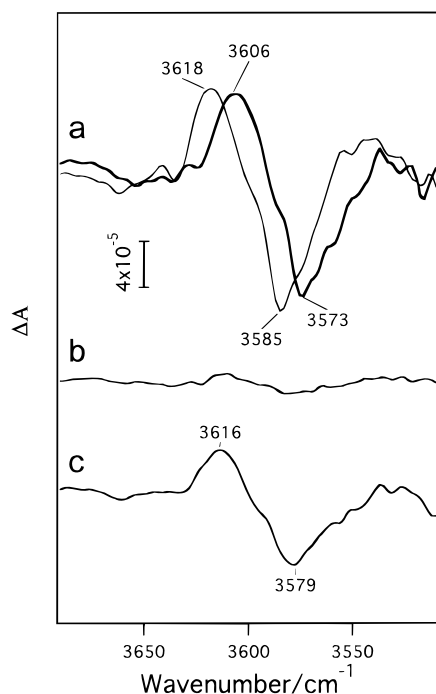


FIGURE 2: S_2/S_1 FTIR difference spectra in the O–H stretching region of PSII core complexes from *S. elongatus* in $H_2^{16}O$ (a, thin line), $H_2^{18}O$ (a, thick line), D_2O (b), and H_2O/D_2O (1:1) (c). Measuring conditions were the same as those for Figure 1. The spectra were normalized to adjust the intensities of the symmetric carboxylate stretching bands at $1403/1362\text{ cm}^{-1}$.

of the peaks at $3618/3585\text{ cm}^{-1}$ shifted to the lower frequencies by 12 cm^{-1} , and the bands are now located at $3606/3573\text{ cm}^{-1}$. This downshift of 12 cm^{-1} is identical to the calculated shift of the O–H frequency upon replacement of ^{16}O by ^{18}O . This observation indicates that the bands at $3618/3585\text{ cm}^{-1}$ both originate from the O–H stretching vibrations of water.

Further evidence was obtained by the measurement of the sample incubated in D_2O . Upon H_2O/D_2O exchange, the bands in the O–H stretching region disappeared as expected (Figure 2b). Instead, in the O–D stretching region, new bands appeared at $2681/2652\text{ cm}^{-1}$ (Figure 3b). The O–D band intensities were smaller than the corresponding O–H intensities (Figures 1a and 2b). This observation is reasonably explained by the molar extinction coefficient of the O–D stretching vibration that is originally smaller than the coefficient of the O–H stretch (41). In H_2O buffer, several successive peaks were detected in this O–D region (Figure 3a) (22). These peaks have already been ascribed to Fermi resonance of the overtones and combinations of the imidazole vibrations with the H-bonded N–H stretch of the histidine ligand of the Mn cluster (22). The peaks reasonably disappeared upon D_2O exchange (Figure 3b). Also, in the S_2/S_1 spectrum in H_2O , a broad background has been observed above 2500 cm^{-1} , which continues up to about 3000 cm^{-1} (partly seen in Figure 3a) (22). The origin of this broad feature was discussed as due to the N–H stretching vibration of the coupled histidine or the O–H or N–H bands of water or proteins that are involved in a H-bonding network around the Mn cluster (22). This broad feature was not affected at all by $H_2^{16}O/H_2^{18}O$ exchange (data not shown), indicating that exchangeable water is not responsible for this feature.

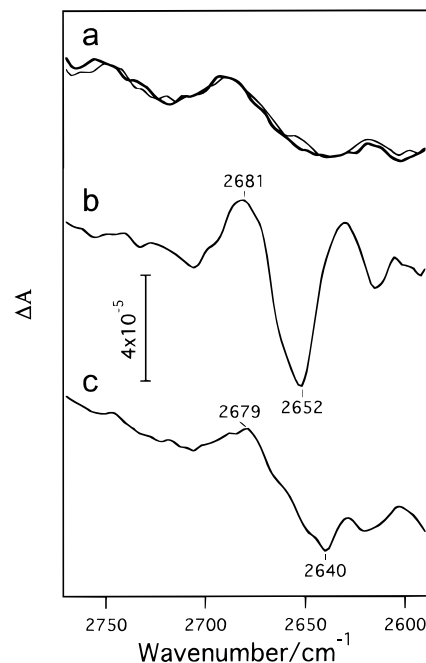


FIGURE 3: S_2/S_1 FTIR difference spectra in the O–D stretching region of PSII core complexes from *S. elongatus* in $H_2^{16}O$ (a, thin line), $H_2^{18}O$ (a, thick line), D_2O (b), and H_2O/D_2O (1:1) (c). Measuring conditions were the same as those for Figure 1. The spectra were normalized to adjust the intensities of the symmetric carboxylate stretching bands at $1403/1362\text{ cm}^{-1}$.

From the above experiments of isotope exchange, it is concluded that the signal at $3618/3585\text{ cm}^{-1}$ arises from the O–H stretching vibrations of a water molecule coupled to the Mn cluster. Upon S_1 -to- S_2 transition, the O–H frequency shifts upward by 33 cm^{-1} from 3585 (S_1) to 3618 cm^{-1} (S_2).

When a water molecule has a symmetric structure, i.e., the two O–H groups have the same interactions, the two O–H vibrations couple with each other, resulting in the asymmetric and symmetric vibrations. The O–H frequency shifts up from the original O–H frequency in the asymmetric vibration and shifts down in the symmetric vibration. For example, in a water molecule in vapor, which takes a symmetric structure, the coupled asymmetric and symmetric vibrations occur at 3756 and 3652 cm^{-1} , respectively (42), with a frequency gap of about 100 cm^{-1} . On the other hand, when a water molecule has an asymmetric structure, this intramolecular coupling is small and each O–H vibration is rather independent. Thus, the structural symmetry of a water molecule can be examined by studying the coupling of the two O–H vibrations. The extent of the O–H coupling is estimated by a frequency shift upon decoupling by partial deuteration of water. Assuming a water molecule, H_1-O-H_2 , the frequency of the O– H_1 stretching vibration coupled with the O– H_2 vibration will shift to the pure O– H_1 frequency by decoupling of the O– H_2 in H_1-O-D_2 . The decoupling shift is larger as the coupling is stronger.

To examine the intramolecular coupling of the O–H bands at $3618/3585\text{ cm}^{-1}$ in the S_2/S_1 spectrum, the spectrum was measured using the PSII sample in a H_2O/D_2O mixture (1:1). Figure 2c shows the O–H stretching region of the spectrum obtained. The band intensities became half of the O–H intensities in H_2O buffer (Figure 1a). [The spectra were normalized at the $1402/1362\text{ cm}^{-1}$ carboxylate bands,

which are not affected by deuteration (19).] The 3618 cm^{-1} band shifted to the lower frequency by 2 cm^{-1} with virtually no change in the bandwidth [20 cm^{-1} in a full width at half-maximum (HWHM)], while the 3585 cm^{-1} band shifted more by 6 cm^{-1} with slight band broadening (from 20 to 26 cm^{-1} in HWHM). In the $\text{H}_2\text{O}/\text{D}_2\text{O}$ (1:1) mixture, four different water species exist with the same amount, i.e., $\text{H}_1\text{—O—H}_2$, $\text{H}_1\text{—O—D}_2$, $\text{D}_1\text{—O—H}_2$, and $\text{D}_1\text{—O—D}_2$. The above spectral changes are explained as that both of the 3618 and 3585 cm^{-1} bands arise from rather isolated O—H modes (defined as O— H_1) with relatively weak intramolecular coupling with O— H_2 . As for the 3585 cm^{-1} band in the S_1 state, the original O— H_1 band in $\text{H}_1\text{—O—H}_2$ is left at 3585 cm^{-1} with a quarter intensity, while the decoupled O— H_1 stretch in $\text{H}_1\text{—O—D}_2$ appears at 3573 cm^{-1} by a 12 cm^{-1} downshift with another quarter intensity, resulting in the broader band centered at 3579 cm^{-1} with a half intensity (Figure 2c). Note that the two bands with a 12 cm^{-1} gap cannot be resolved because of the original bandwidth of 20 cm^{-1} . The coupling of the 3618 cm^{-1} band in the S_2 state is much smaller; the frequency shift upon decoupling is predicted to be only 4 cm^{-1} , resulting in the apparent 2 cm^{-1} shift due to the overlap of the original band of $\text{H}_1\text{—O—H}_2$ at 3618 cm^{-1} and the decoupled band of $\text{H}_1\text{—O—D}_2$ at 3614 cm^{-1} . The bandwidth is virtually unchanged because of this small shift.

Similar spectral changes, i.e., half-band intensities and downshifts of the peak positions with a larger shift in the S_1 band, were seen in the O—D stretching region (Figure 3c in comparison with Figure 3b). Unfortunately, band features are less clear due to the background slope and some superimposing structures. Nevertheless, this observation confirms the above view of intramolecular coupling of the observed water molecule.

DISCUSSION

We have observed the vibrations of a water molecule coupled with the reaction of the WOC. In the S_2/S_1 FTIR difference spectrum, the positive and negative bands at 3618 and 3585 cm^{-1} , respectively, were definitely assigned to the O—H stretching vibrations of the water by H_2^{18}O and D_2O substitutions (Figures 2 and 3).

The free O—H vibration of H_2O in vapor occurs at 3704 cm^{-1} [the mean value of the coupled asymmetric and symmetric stretching vibrations at 3756 and 3652 cm^{-1} (42)]. The O—H vibration shifts to the lower frequency upon H-bonding, and thus the O—H frequency is a good indication of H-bonding strength (27–33). For example, weak H-bonding to acetonitrile shows a downshift ($\Delta\nu$: $\nu_{\text{free}} - \nu_{\text{H-bond}}$) by $50\text{--}140\text{ cm}^{-1}$ depending on solvents, while strong H-bonding to triethylamine gives $\Delta\nu = \sim 450\text{ cm}^{-1}$ (31). In a water dimer, the H-bonded O—H shows a $\Delta\nu$ of $100\text{--}160\text{ cm}^{-1}$ (32, 33), while liquid water or water clusters show stronger H-bonds with $\Delta\nu$ as much as $300\text{--}500\text{ cm}^{-1}$ due to the cooperativity effect of H-bonding networks (29, 32, 33). Metal binding to the oxygen atom of water also tends to increase $\Delta\nu$ (28, 29).

The O—H bands of water in the WOC at $3618/3585\text{ cm}^{-1}$ (S_2/S_1 states) (Figure 2) give $\Delta\nu$ values of $86/119\text{ cm}^{-1}$ ($90/131\text{ cm}^{-1}$ if $\Delta\nu$ is calculated using the decoupled O—H frequencies of $3614/3573\text{ cm}^{-1}$; see below). These values

indicate that the observed O—H group is weakly H-bonded in both the S_1 and S_2 states. The upshift of the O—H frequency by 33 cm^{-1} (41 cm^{-1} in the decoupled O—H) upon S_2 formation means that the H-bonding interaction of this O—H group becomes weaker in this process.

The decoupling experiment by measuring the spectrum in $\text{H}_2\text{O}/\text{D}_2\text{O}$ (1:1) provided the information of the intramolecular coupling of the observed O—H vibration with another O—H in the H_2O molecule (Figure 2c). The extent of the coupling was estimated as the shift upon decoupling, and values of 4 and 12 cm^{-1} were obtained for the 3618 and 3585 cm^{-1} bands, respectively. These values are much smaller than 52 cm^{-1} for free water in vapor that has a symmetric structure (42). This small O—H coupling indicates a significantly asymmetric structure of the water in the WOC. Because no prominent bands were observed in the higher frequency side of the $3618/3585\text{ cm}^{-1}$ bands up to 3800 cm^{-1} (Figure 1a), the other coupled O—H bands should be located in the strongly H-bonded O—H region below 3500 cm^{-1} . The observation that the $3618/3585\text{ cm}^{-1}$ bands downshifted upon decoupling (Figure 2c) supports this idea, because the higher frequency O—H band is shifted up by coupling, that is, shifted down by decoupling. It is concluded, therefore, that the observed water has an asymmetric structure in which one O—H is weakly H-bonded, whereas the other O—H is strongly H-bonded. Unfortunately, this strongly H-bonded O—H band could not be identified in this study, because the frequency region at $3500\text{--}3100\text{ cm}^{-1}$, where the band is expected to be found, was not measurable due to the absorption saturation by bulk water (Figure 1, inset).

The observation that the O—H coupling is smaller in the S_2 state (4 cm^{-1}) than in the S_1 state (12 cm^{-1}) indicates that this H_2O has a more asymmetric structure in the S_2 state. This probably resulted from the further weakened H-bonding of the weakly H-bonded O—H group in the S_2 state as seen in the 33 cm^{-1} upshift. In this case, the strong H-bonding of the other O—H group may be strengthened more by the anticooperativity effect (30); i.e., when the H-bonding of one O—H is strengthened, that of the other O—H is weakened, and vice versa. It may also be possible, on the contrary, that the 33 cm^{-1} upshift is the result of the anticooperativity of the strengthened H-bond of the other O—H. In any case, the structural symmetry of the water is lowered, resulting in the smaller coupling between the two O—H groups. It is worth noting that because the intramolecular coupling of the O—H vibrations was observed in both the S_1 and S_2 states, the possibility that the observed O—H bands arise from a hydroxyl form (OH^- anion or OH^\bullet radical) can be excluded.

The relatively large upshift of the O—H stretching frequency by 33 cm^{-1} upon S_2 formation and the structural changes discussed above indicate that this water molecule is strongly coupled to the reaction of the WOC. Also, the observed weak H-bonding shows that this water is located rather isolated from bulk water. Therefore, the primary candidate for this water is substrate water that is directly coordinated to the Mn cluster. In this case, the observation in the present study indicates that at least one water molecule is coordinated to Mn in both the S_1 and S_2 states, being consistent with the conclusion from the ESEEM study by Britt (2). Previously, we suggested, from the large upshift of an asymmetric carboxylate stretching band upon H/D exchange, the presence of a water ligand strongly H-bonded

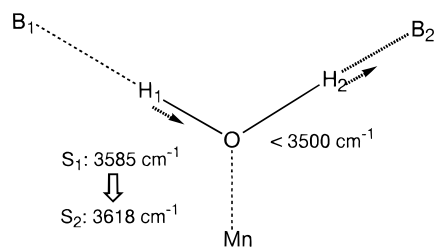


FIGURE 4: Proposed structure of the water molecule in the WOC detected in the FTIR spectra. B_1 and B_2 , which are unknown H-bond acceptors, form weak and strong H-bonds with H_1 and H_2 , respectively. Dotted arrows indicate the directions of the structural changes upon S_1 -to- S_2 transition.

to the carboxylate ligand (19). It is possible that this water ligand is the one that we have detected in the present study. If this is the case, we have probably observed the O–H group other than the O–H that is interacting to the carboxylate group.

The observed water molecule is not deprotonated upon S_1 -to- S_2 transition. However, its structure becomes more asymmetric and probably the strongly H-bonded O–H becomes more acidic in the S_2 state. It is conceivable that such a structural change facilitates the release of this acidic proton in the later step, by lowering the potential barrier. It should be noted that the Mn ion that binds the observed water may not be the one that is directly oxidized from III to IV upon S_2 formation (3, 7). If the water were coordinated to the oxidized Mn, the O–H frequency would decrease due to H-bond cooperativity of the metal ion (28, 29), which should be larger in Mn(IV) than in Mn(III). A hypothetical view is that the water-binding Mn is oxidized in the next S_2 -to- S_3 transition, making the strongly H-bonded proton further acidic, and then the proton is finally liberated. The proposed structure of the water ligand observed in this study is depicted in Figure 4.

Although the above structure of Mn-bound water is most plausible at the moment, direct evidence for this structure must be obtained by detection of the Mn–H₂O vibrations, which occur in the low-frequency region ($<700\text{ cm}^{-1}$) (43).² Therefore, the possibility that the observed water is not a direct ligand of Mn cannot be excluded. Even in this case, this water molecule should be located in the vicinity of the Mn cluster and strongly coupled to it through a H-bonding network. Hence, the water can still be a substrate, which is not bound to the Mn in the S_1 and S_2 states but is incorporated into the ligand sphere in the S_3 or S_4 state. Another possibility is that this water is in the proton-transfer pathway and functions as a proton-transfer mediator. In fact, such water molecules that play important roles in proton-transfer reactions have been found in bacteriorhodopsin and rhodopsin by FTIR spectroscopy (34, 35).

We probably detected one of the two substrate water molecules. The other substrate water may have strong H-bonding in both the O–H groups, so that the band would

occur in the strongly H-bonded O–H region that we could not detect in this study. It seems unlikely that the observed bands are the overlap of the two water molecules, because in this case these two waters must have the same molecular interactions in both the S_1 and S_2 states. Further studies of the FTIR measurements in the strongly H-bonded O–H region using dried PSII samples would be necessary to clarify the H-bonding structures of both of the substrate water molecules.

In conclusion, we have detected, for the first time, the vibrations of an active water molecule, probably substrate water, in the WOC by FTIR spectroscopy. The analysis of the bands showed that this water molecule has an asymmetric structure, in which one of the O–H groups is weakly H-bonded whereas the other is strongly H-bonded. Upon S_2 formation, the H-bonding structure becomes more asymmetric. It was assumed that this structural change decreases a potential barrier of the proton release reaction in the later step. The present study showed that FTIR detection of the O–H stretching vibrations of water is a very useful and promising method to directly monitor the chemical reactions of substrate water and clarify the molecular mechanism of the water-oxidizing process in the WOC.

ACKNOWLEDGMENT

We thank Professor Akio Maeda and Dr. Hideki Kandori for precious discussion about the water detection by FTIR spectroscopy. We also thank Dr. Yorinao Inoue for kind support of this study.

REFERENCES

1. Debus, R. J. (1992) *Biochim. Biophys. Acta* 1102, 269–352.
2. Britt, R. D. (1996) in *Oxygenic Photosynthesis: The Light Reactions* (Ort, D. R., and Yocum, C. F., Eds.) pp 137–164, Kluwer, Dordrecht, The Netherlands.
3. Yachandra, V. K., Sauer, K., and Klein, M. P. (1996) *Chem. Rev.* 96, 2927–2950.
4. Renger, G. (1997) *Physiol. Plant.* 100, 824–841.
5. Rüttiger, W., and Dismukes, G. C. (1997) *Chem. Rev.* 97, 1–24.
6. Tommos, C., and Babcock, G. T. (1998) *Acc. Chem. Res.* 31, 18–25.
7. Yachandra, V. K., DeRose, V. J., Latimer, M. J., Mukerji, I., Sauer, K., and Klein, M. P. (1993) *Science* 260, 675–679.
8. Sharp, R. R. (1992) in *Manganese Redox Enzymes* (Pecoraro, V. L., Ed.) pp 177–196, VCH Publishers, New York.
9. Messinger, J., Badger, M., and Wydrzynski, T. (1995) *Proc. Natl. Acad. Sci. U.S.A.* 92, 3209–3213.
10. Hansson, Ö., Andreasson, L.-E., and Vänngård, T. (1986) *FEBS Lett.* 195, 151–154.
11. Nugent, J. H. A. (1987) *Biochim. Biophys. Acta* 893, 184–189.
12. Turconi, S., MacLachlan, D. J., Bratt, P. J., Nugent, J. H. A., and Evans, M. C. W. (1997) *Biochemistry* 36, 879–885.
13. Kawamori, A., Inui, T., Ono, T., and Inoue, Y. (1989) *FEBS Lett.* 254, 219–224.
14. Fiege, R., Zweggart, W., Bittl, R., Adir, N., Renger, G., and Lubitz, W. (1996) *Photosynth. Res.* 48, 227–237.
15. Tang, X.-S., Sivaraja, M., and Dismukes, G. C. (1993) *J. Am. Chem. Soc.* 115, 2382–2389.
16. Noguchi, T., Ono, T., and Inoue, Y. (1992) *Biochemistry* 31, 5953–5956.
17. Noguchi, T., Ono, T., and Inoue, Y. (1993) *Biochim. Biophys. Acta* 1143, 333–336.
18. Noguchi, T., Ono, T., and Inoue, Y. (1995) *Biochim. Biophys. Acta* 1228, 189–200.
19. Noguchi, T., Ono, T., and Inoue, Y. (1995) *Biochim. Biophys. Acta* 1232, 59–66.

² After submission of this paper, the authors noticed that the study of low-frequency resonance Raman spectra of the Mn cluster by Cua et al. (44) was published very recently. They observed several Raman bands in the 500–300 cm^{-1} region sensitive to $\text{D}_2\text{O}/\text{H}_2\text{O}$ exchange in the S_1 state and attributed these bands to Mn–H₂O/OH[−] vibrations. Although definitive assignments of these bands await $^{18}\text{O}/^{16}\text{O}$ exchange, it is possible that the bands include the low-frequency vibrations of the water molecule observed in the present study.

20. Noguchi, T., and Inoue, Y. (1995) *J. Biochem.* 118, 9–12.
21. Noguchi, T., Inoue, Y., and Tang, X.-S. (1997) *Biochemistry* 36, 14705–14711.
22. Noguchi, T., Inoue, Y., and Tang, X.-S. (1999) *Biochemistry* 38, 10187–10195.
23. Noguchi, T., Sugiura, M., and Inoue, Y. (1999) in *Fourier Transform Spectroscopy* (Itoh, K., and Tasumi, M., Eds.) pp 459–460, Waseda University Press, Tokyo, Japan.
24. Onoda, K., Mino, H., Inoue, Y., and Noguchi, T. (2000) *Photosynth. Res.* 63, 47–57.
25. Zhang, H., Fischer, G., and Wydrzynski, T. (1998) *Biochemistry* 37, 5511–5517.
26. Chu, H.-A., Gardner, M. T., O'Brien, J. P., and Babcock, G. T. (1999) *Biochemistry* 38, 4533–4541.
27. Pimentel, G. C., and McClellan, A. L. (1960) in *The Hydrogen Bond*, W. H. Freeman, San Francisco.
28. Kleeberg, H., Heinje, G., and Luck, W. A. P. (1986) *J. Phys. Chem.* 90, 4427–4430.
29. Kleeberg, H., and Luck, W. A. P. (1989) *Z. Phys. Chem. (Leipzig)* 270, 613–625.
30. Luck, W. A. P., Klein, D., and Rangswatnananon, K. (1997) *J. Mol. Struct.* 416, 287–296.
31. Luck, W. A. P., and Klein, D. (1996) *J. Mol. Struct.* 381, 83–94.
32. Xantheas, S. S., and Dunning, T. H., Jr. (1993) *J. Chem. Phys.* 99, 8774–8792.
33. Huisken, F., Kaloudis, M., and Kulcke, A. (1996) *J. Chem. Phys.* 104, 17–25.
34. Maeda, A., Kandori, H., Yamazaki, Y., Nishimura, S., Hatanaka, M., Chon, Y.-S., Sasaki, J., Needleman, R., and Lanyi, J. K. (1997) *J. Biochem.* 121, 399–406.
35. Kandori, H. (2000) *Biochim. Biophys. Acta* (in press).
36. Sugiura, M., and Inoue, Y. (1999) *Plant Cell Physiol.* 40, 1219–1231.
37. Berthomieu, C., Navedryk, E., Mantele, W., and Breton, J. (1990) *FEBS Lett.* 269, 363–367.
38. Hienerwadel, R., Boussac, A., Breton, J., and Berthomieu, C. (1996) *Biochemistry* 35, 15447–15460.
39. Hienerwadel, R., and Berthomieu, C. (1995) *Biochemistry* 34, 16288–16297.
40. Hienerwadel, R., and Berthomieu, C. (1995) in *Photosynthesis: from Light to Biosphere* (Mathis, P., Ed.) Vol. 1, pp 743–746, Kluwer, Dordrecht, The Netherlands.
41. Vennyaminov, S. Y., and Prendergast, F. G. (1997) *Anal. Biochem.* 248, 234–245.
42. Herzberg, G. (1945) in *Molecular Spectra and Molecular Structure, II. Infrared and Raman Spectra of Polyatomic Molecules*, p 281, van Nostrand, Princeton, NJ.
43. Nakamoto, K. (1997) in *Infrared and Raman Spectra of Inorganic and Coordination Compounds*, Part B, 5th ed., pp 53–57, John Wiley & Sons, New York.
44. Cua, A., Stewart, D. H., Reifler, M. J., Brudvig, G. W., and Bocian, D. F. (2000) *J. Am. Chem. Soc.* 122, 2069–2077.

BI001040I